Published in final edited form as:
Small. 2012 October 22; 8(20): 3143–3150. doi:10.1002/smll.201200783.

Hollow Copper Sulfide Nanoparticle-Mediated Transdermal Drug Delivery

Mr. Samy Ramadan, **Dr. Liangran Guo**, **Mrs. Yajuan Li**, **Prof. Bingfang Yan**, and **Prof. Wei Lu**[*]
Department of Biomedical and Pharmaceutical Sciences University of Rhode Island 41 Lower College Road, Kingston, RI 02881 (USA)

Abstract

Nanoparticles with strong optical absorption at near-infrared (NIR) wavelengths can efficiently convert optical energy into thermal energy, and have shown multimodality in biological and biomedical applications. In this work, a new type of thermal ablation-enhanced transdermal delivery methodology is developed based on hollow copper sulfide nanoparticles (HCuSNPs) with intense photothermal coupling effects. Application of nanosecond-pulsed NIR laser allows rapid heating of the nanoparticles and instantaneous heat conduction. This provides very short periods of time but extremely high temperatures (estimated over 100°C) in local regions, with focused thermal ablation of the stratum corneum. Because the discontinuous light from the pulsed laser minimized heat accumulation, the average temperature of the irradiated skin area only increases to ~40–50°C. The extent of thermal ablation of skin, i.e. removal of the stratum corneum, viable epidermis, or the dermis, can be controlled by adjusting the laser power. The skin disruption by HCuSNP-mediated photothermal ablation significantly increases the permeability of macromolecule drugs such as human growth hormone, providing effective and controlled percutaneous delivery. This technique offers compelling opportunities to overcome low oral bioavailability of small- and large-molecular-weight drugs, avoiding the pain and inconvenience of long-term s.c. injections while enabling sustained and controlled delivery.

Keywords

nanoparticle; transdermal; drug delivery; near-infrared laser; photothermal ablation

1. Introduction

Transdermal delivery has been an attractive route of drug administration and made an increasing contribution to medical practice. It can provide sustained and steady-state pharmacokinetics, address issues of low oral bioavailability, avoid hepatic first-pass effects, and improve the patient compliance.[1] However, traditional transdermal patches used in most clinical products have been limited to lipophilic drugs with the molecular weight less than a few hundred Daltons.[2] Due to the presence of lipid-rich stratum corneum barrier, percutaneous delivery of hydrophilic macromolecules such as peptides and proteins presents a difficult challenge.[3] In pursuit of overcoming this limitation, a variety of physically enhanced transdermal technologies have been developed to disrupt the stratum corneum such as microneedles,[4] thermal ablation,[5] microdermabrasion,[6] electroporation[7] and cavitational ultrasound.[8] Among them, thermal ablation technology represents an attractive advance in recent years. This technology is principled to directly heat skin surface to

[*]weilu@uri.edu.

generate micron-scale perforations in the stratum corneum, mainly through microheaters,[5b] radio-frequency[5c, 5d] or laser.[5e, 5f] All these approaches rely on precise control over the skin disruption to minimize the injury to the surrounding and deeper tissue.

Photothermal nanoparticles are engineered particles possessing a photothermal coupling effect. For example, gold nanostructures such as nanoshells,[9] nanorods,[10] nanocages,[11] and hollow nanospheres[12] have unique optical properties due to strong and tunable surface plasmon resonance (SPR). They can be fabricated to absorb near-infrared (NIR) light (650–900 nm), resulting in resonance and transfer of thermal energies to the surrounding tissue to raise the temperature.[9, 13] The absorbance of NIR light is desirable because it causes minimal thermal injury to normal tissues with optimal light penetration.[14] The photothermal effect by the gold nanoparticles can be utilized for photothermal ablation therapy of tumor cells,[15] as well as NIR laser triggered-release of various agents such as small molecules,[16] DNAs,[17] and small interfering RNAs.[18] Moverover, a surfactant/protein/gold nanorod complex has been applied to transdermal delivery of proteins.[19]

Semiconductor CuS nanoparticles (CuSNPs) are a new class of photothermal nanoparticles that provide an alternative to gold analogs. Unlike the optical absorption in gold nanostructures based on the SPR,[20] the NIR light absorption of CuSNPs derives from the *d-d* transition of Cu^{2+} ions.[21] The SPR peak of gold nanostructures is dependent on the dielectric constant of the surrounding medium.[22] Therefore, the absorption wavelength of gold nanostructures will be altered by the solvent or the surrounding environment when they are formulated or delivered *in vivo*.[19, 21] In contrast, the absorption wavelength of CuSNPs is not affected.[21] Further, compared to gold, CuS is much less expensive.[21] Irradiated with NIR laser, CuSNPs generated heat with photothermal destruction of tumor cells both *in vitro*[21] and *in vivo* through intratumor[23] or intravenous injection.[24]

In this study, we design a hollow copper sulfide nanoparticle (HCuSNP)-mediated transdermal delivery technique. We hypothesize that the photothermal conversion of the HCuSNPs could be harnessed to promote controlled thermal ablation of the stratum corneum through heat conduction in order to enhance drug permeability (Scheme 1). Application of nanosecond-pulsed NIR laser would provide very short periods of time but extremely high temperatures in local regions, with focused thermal ablation of the stratum corneum, limiting heat transfer to deep tissue. We expect that the extent of thermal ablation of skin, i.e. removal of stratum corneum, viable epidermis, or dermis, would be controlled by adjusting the laser power.

2. Results and Discussion

Transmission electron micrograph shows that the HCuSNPs are hollow and core-shell spheres with an average diameter around 55 nm (Figure 1A). The nanoparticles have an optical absorption band peaking at 1050 nm, with ~80% of peak absorbance intensity at 900 nm of NIR wavelength (Figure 1B).

To be topically applied to the skin of nude mice, the HCuSNPs were suspended in Carbomer 940 hydrogel. Carbomer 940 approved by United States Pharmacopeia has been used in various transdermal drug delivery systems. The function of Carbomer 940 here is to increase the viscosity of the formulation. Propylene glycol (10%) was contained in the gel formula serving as wetting agents to increase the surface contact between the gel and the skin. After the skin was heated with a light bulb for 20 min, the water in the gel evaporated and the nanoparticles were well deposited on the surface of the stratum corneum. The HCuSNP-coated skin was then irradiated with neodymium:yttriumaluminum-garnet (Nd:YAG) laser in tandem with Ti:sapphire laser, whose wavelength was set at 900 nm. Real time infrared thermal imaging was used to monitor the skin temperature pre-, intra- and post- NIR laser

irradiation. Figure 2 depicts the temperature of the skin area pretreated with HCuSNP gel elevated immediately after laser irradiation. The temperature continued to increase with laser exposure time. It reached plateaus of 40°C and 50°C after laser treatment for 5 s with power intensities of 1.3 W/cm^2 and 2.6 W/cm^2, respectively. Thus, the duration of laser treatment for all following experiments was set at 5 s. The blank gel without HCuSNPs did not increase the skin temperature even at high power (2.6 W/cm^2).

The effect of NIR laser treatment on nude mouse skin *in vivo* with or without HCuSNPs was evaluated by histology studies (Figure 3). Without laser treatment, the HCuSNP gel did not induce any histological change of the skin (Figure 3A). The blank gel-applied skin remained intact after NIR laser irradiation at 2.6 W/cm^2 (Figure 3B). However, significant histological changes were observed in HCuSNP gel-applied skin following laser treatment. Figure 3C illustrates removal or stripping the stratum corneum from the epidermis by NIR laser at 1.3 W/cm^2. This damage was confined to the stratum corneum layer without damage to the viable epidermis. The pore depth was measured as 11±2 μm from 10 hematoxylin & eosin (H&E)-stained slices. Increasing the laser power to 2.6 W/cm^2 resulted in thermal ablation penetrating into the viable epidermis, reaching the epidermal-dermal junction and creating deeper pores that extended into the dermis (Figure 3D). The pore depth was measured as 29±7 μm (n=10). The application of HCuSNP solution without gel following laser treatment showed similar ablation effect on the skin compared with HCuSNP gel (Figure 3E compared to 3C; Figure 3F compared to 3D), indicating the use of gel on skin surface did not affect the energy efficiency of NIR laser.

To provide more detailed information of the changes in stratum corneum, the laser-treated skin was stained with the lipid-soluble fluorescent dye, Nile red (Figure 4).[25] Mouse skin applied with HCuSNP gel alone maintained a high degree of alignment of intercellular lipids in the stratum corneum with well-ordered stacking arrangement of corneocytes, suggesting the HCuSNP gel itself did not alternate the structure of the stratum corneum (Figure 4A and inner graph). In addition, mouse skin treated with blank gel plus high powered laser (2.6 W/cm^2) did not display significant changes in the integrity of the stratum corneum (Figure 4B and inner graph). However, mouse skin exposed to the HCuSNP gel plus low powered laser treatment (1.3 W/cm^2) had a highly disordered stratum corneum, which was absent in certain areas (Figure 4C, arrowheads). This could be attributed to breaking of the stratum corneum keratin network.[5a] In mouse skin treated with HCuSNP gel plus high powered laser (2.6 W/cm^2), the stratum corneum was extensively damaged and densely packed, with little of its original structure remaining (Figure 4D, asterisk and inner graph). Some of the stratum corneum and partial epidermis structure disappeared (Figure 4D, arrow), probably due to heat-induced chemical decomposition of the tissue.[5a] Park et al reported that heating the skin with short and high temperature pulses sequentially induced a stratum corneum densely packed, disordered, and broken down as a result of the increase of temperature from 100°C to 315°C.[5a] Our results are consistent with such changes induced by the local heat, indicating the thermal conduction from the HCuSNPs triggered by the pulsed Nd:YAG laser to the skin could lead to focused and instantaneous temperatures exceeding 100°C.

Compared with the continuous-wave (CW) laser power (12 W/cm^2) previously used in CuS nanoparticle-mediated photothermal ablation therapy,[24] the Q-switched pulsed laser of less than 15 ns per pulse applied here (1.3 and 2.6 W/cm^2) has less average power. However, the peak power of the pulsed laser greatly exceeds that of the CW laser.[26] Thus, the pulsed laser induces very effective local heating by photo-excitation.[26] Our histological results proved that pulse irradiation of the HCuSNP-applied mouse skin for only 5 s was sufficient to locally destroy the stratum corneum and even the viable epidermis. Whereas, previous report indicated that CuS nanoparticle-mediated photothermal ablation of cancer cells required a 5-minute exposure to CW laser at a higher power.[24] Unlike CW laser generating

continuous laser light, the pulsed laser creates discontinuous light (pulse repetition rate of 10 Hz) and produces instantaneous heating. Such heating ceases at the end of each light pulse, resulting in much less temperature increase in the skin compared to CW laser. Accordingly, HCuSNP-mediated thermal ablation of the skin induced by the Nd:YAG laser raised the average skin temperature at the site of exposure to only ~40–50°C.

For thermal ablation-enhanced transdermal drug delivery, keeping the thermal exposure in sufficiently short periods of time is important. This mode of heating enables the temperature gradient across the stratum corneum to be steep enough that the skin surface is extremely hot but not the viable epidermis and deeper skin tissues.[27] Therefore, “cold ablation” can be done with high energy short duration laser pulses (microseconds or less) with limited or negligible heat transfer to surrounding tissue.[27] Alternatively, in the previously reported transdermal drug delivery system enhanced by the solid-in-oil dispersion of gold nanorods, a xenon lamp was used as continuous NIR light source that required high light power (6 W/cm^2) and long duration of light exposure (20 min) to ablate the stratum corneum,[19] causing extremely high energy (7200 J/cm^2). This is 3-order of magnitude higher than the pulsed laser energy used in our system, which was 6.5 J/cm^2 with laser power density of 1.3 W/cm^2 for 5 s exposure time. Therefore, the heat propagation to deep surrounding tissue using light source from xenon lamp could be a major concern.

To measure the change of transdermal flux after HCuSNP gel and NIR laser pretreatment, we used fluorescein isothiocyanate-labeled dextran (dextran-FITC, MW 20 k) to examine the skin penetration of the hydrophilic macromolecules. In mice pretreated with HCuSNP gel alone or with blank gel plus NIR laser, the fluorescence of dextran-FITC stayed on the surface of the skin (Figures 5A and 5B). However, in mice pretreated with HCuSNP gel plus low powered NIR laser (1.3 W/cm^2), green fluorescence was observed throughout the epidermis with further penetration into dermis layer (Figure 5C). Application of HCuSNP gel plus high powered laser (2.6 W/cm^2) caused partial disappearance of the epidermis, which allowed the dextran-FITC to penetrate deeper into the dermis (Figure 5D).

We next chose human growth hormone (hGH), a 22-kDa protein of 191 amino acids, to test the percutaneous delivery of macromolecular drugs by the HCuSNP-mediated photothermal ablation technique in comparison with chemical enhancement approach — a conventional enhancement technique used in transdermal patches. *In vitro* permeation results as shown in Figure 6A illustrate that application of chemical enhancer 5% Azone increased the skin permeability to hGH [$(1.7\pm0.3)\times10^{-5}$ cm/h] by ~6.3-fold compared to that of skin without pretreatment [$(2.7\pm0.4)\times10^{-6}$ cm/h]. Skin pretreated with HCuSNP gel alone [$(2.6\pm0.6)\times10^{-6}$ cm/h] or laser (2.6 W/cm^2) alone [$(2.9\pm1.1)\times10^{-6}$ cm/h] did not show permeability enhancement. In contrast, HCuSNP-mediated photothermally ablated skin displayed a remarkable increase in the transdermal flux of hGH. In group of skin pretreated with HCuSNP gel plus NIR laser (1.3 W/cm^2), skin permeability to hGH was $(2.3\pm0.5)\times10^{-3}$ cm/h. Increase of laser power to 2.6 W/cm^2 enhanced ~26% of the permeation rate [$(2.9\pm0.3)\times10^{-3}$ cm/h]. Compared with ~6.3-fold increase in permeability to hGH by chemical enhancer Azone, HCuSNP-mediated photothermal ablation technique increased the permeability by about 3-order of magnitude as high as that of untreated skin. The penetration of hGH across the photothermally ablated skin had a lag time of 5.4±0.7 h (1.3 W/cm^2 of laser power) or 4.5±0.5 h (2.6 W/cm^2 of laser power). This is attributed to the use of full-thickness mouse skin for *in vitro* study providing a whole dermis layer for drug molecules to permeate. However, for drug delivery *in vivo* a drug needs only to penetrate to the capillary bed in the superficial dermis for systemic delivery.[27a] Therefore, permeability could be significantly larger and lag time could be remarkably shorter *in vivo*.[27a]

Figure 6B depicts serum hGH levels in nude mice after s.c. injection or transdermal delivery of 10 μg of hGH. Following s.c. injection, serum hGH levels quickly reached a peak, with an average concentration of 60 ng/ml at 30 min, returning to baseline at 4 h. For transdermal delivery, after receiving different pretreatments, mice were topically applied with hGH gel for 3 h starting at time 0. In mice pretreated with HCuSNP gel alone or gel without HCuSNPs plus NIR laser, nearly no percutaneous absorption of hGH was detected. Transdermal delivery of hGH using the HCuSNP-mediated photothermal ablation technique significantly increased serum drug concentration with an average bioavailability of 70% (1.3 W/cm^2 of laser power) or 83% (2.6 W/cm^2 of laser power) relative to that of the s.c. injection. There was only 13% of the bioavailability difference in the mouse groups treated with HCuSNP gel plus laser between high (2.6 W/cm^2) and low (1.3 W/cm^2) power intensity, while deeper skin disruption with high power laser was found in histology. This result indicates the major diffusional barriers to transport of hGH is the stratum corneum. After removal of the stratum corneum layer, either the viable epidermis or the dermis has minor effect on hGH transport. Unlike s.c. injection, the transdermal delivery of hGH did not produce an abrupt peak at 30 min. Instead, a relatively slower absorption of hGH following percutaneous delivery generated a relatively flat drug concentration-time curve, which delayed the peak time until 2–3 h and extended the duration of effective serum drug concentrations. The peak concentration of hGH via percutaneous delivery was only one third of that produced by s.c. delivery, reducing the risk of adverse effects related to high concentrations. In comparison with photothermal ablation enhancement, the transdermal delivery of hGH using the chemical enhancer 5% Azone only had a bioavailability of ~2.7% relative to that of the s.c. injection.

In HCuSNP-mediated photothermal ablation technique, the nanoparticles were applied on the skin surface serving as enhancers. They were removed after laser treatment. Thus, we applied HCuSNPs with or without gel on BALB/c mouse ears once a day for three consecutive days to test the potential irritancy of HCuSNPs on skin. Ear swelling[28] was evaluated by measuring the ear thickness before the nanoparticle application and 24 h after the last exposure. A 0.3% of 2,4-dinitrofluorobenzene (DNFB) was used as a positive control for irritancy studies[28] and resulted in an average significant increase of 92% ear swelling after the application (Figure 7A). However, there was no significant ear swelling in HCuSNPs with or without gel treatment group compared with untreated control. This result was further confirmed by histological analysis (Figure 7B). In mouse ears treated with DNFB, epidermal hyperplasia and intra-epidermal inflammatory cell infiltration in the superficial dermis was observed. There was no significantly histological change of mouse ears treated with HCuSNPs with or without gel compared to the untreated ears. These data demonstrated that either HCuSNPs or HCuSNP gel have little or no irritancy on skin.

The success of photothermal ablation enhancement approach relies on the highly photothermal coupling efficiency of the HCuSNPs at NIR wavelength region. Application of very short (femtosecond to nanosecond) pulsed NIR laser allows large amount of energy to be tightly packed in the laser pulses,[26] producing rapid heating in the nanoparticles.[29] In this case, the temperature of nanoparticles could be raised by several hundred degrees.[30] This is followed by rapid heat transfer out of the particle to the surrounding tissues and quick cooling of the nanoparticles at the end of each laser pulse.[29] Instantaneous heat conduction could allow increase in temperature exceeding 100°C to be localized. Because the discontinuous light of the pulsed laser causes less heat accumulation than CW laser, the average temperature of the irradiated skin area only increases to ~40–50°C. Nevertheless, this kind of heat conduction could cause disordering of stratum corneum lipid structure, disruption of stratum corneum keratin network structure, or decomposition and vaporization of keratin to micron-scale holes in the stratum corneum.[5a] The disrupted skin surface

subsequently allows substantial absorption of macromolecules. A proposed mechanism is shown in Scheme 1.

Our current work demonstrated that an NIR laser-activated transdermal drug delivery mediated by HCuSNPs is an effective large-molecule-drug delivery technique. The comparative study proved this photothermal ablation enhancement has advantage of permeability to macromolecules over chemical enhancement (Figure 6). The permeability enhancement by chemical enhancers is caused by interference with the packing arrangement of the intercellular lamellar lipids in the stratum corneum through insertion of amphiphilic molecules into the lipid bilayers,[31] or by extracting lipids using solvents and surfactants to create lipid packing defects of nanometer dimensions.[2] Therefore, chemical enhancement is limited to small, lipophilic molecules and has limited effect on larger or hydrophilic molecules.[2] In contrast, the photothermal ablation approach increases the skin permeability to 22-kDa hGH by 3-fold of magnitude (Figure 6A). It was reported that thermal ablation-enhancement techniques made micrometer dimensions of disruptions to the stratum corneum structures.[2] These micro-scale disruptions created channels of sufficient dimensions for passage of macromolecules including antibodies.[27b] Therefore, it is believed that HCuSNP-mediated photothermal ablation enhancement technique is able to be used for transdermal delivery of drugs with molecular weight lager than 22 kDa. The photothermal ablation-induced micro-scale disruptions are also ideal for antigen delviery. Transdermal delivery of vaccine targets the potent epidermal Langerhans and dermal dendritic cells that generate a strong immune response at much lower doses than hypodermic injection.[32] Furthermore, the photothermal nanoparticles can not only serve as a permeation enhancer but also provide a platform for co-delivery of therapeutic drugs.

It is worth noting that by modulating the NIR laser power it is possible to control the degree of thermal ablation — to remove only the stratum corneum, to reach the viable epidermis, or to penetrate the dermis. Although the deeper damage to the skin increases the drug delivery, successful transdermal delivery depends on balancing effective delivery with safety to the skin. The openings of the stratum corneum are temporary, since this layer is continually replaced through the natural process of desquamation.[5b] Based on the data from clinical trials of microneedle and thermal ablation-enhanced transdermal delivery, relatively large and micron-scale defects in the stratum corneum are considered as well-tolerated by patients as long as significant damage is not done to living cells in the viable epidermis and dermis.[2] The results of Figures 3 and 5 show that our technique makes it possible to selectively remove the stratum corneum without entering the deeper viable epidermis, by precisely adjusting the laser power while maintaining the effective drug delivery. The long-term safety of this technique to the skin will be examined in future studies.

3. Conclusion

In summary, we described a HCuSNP-mediated transdermal delivery methodology. This technique is built on the unique optical property of the nanoparticles that display strong absorbance in the NIR region and mediate intense photothermal conversion effects. The applied nanosecond-pulsed NIR laser provided very short periods of time but extremely high temperatures in local regions, with focused thermal ablation of the stratum corneum. Success of this technique could enable sustained and controlled transdermal delivery of both small molecules and macromolecules with low oral bioavailabilities avoiding the pain and inconvenience of long-term s.c. injections.

Experimental Section

Materials—The chemicals used were purchased from Sigma-Aldrich Chemical, Inc. unless mentioned specifically. Nude mice and BALB/c mice (both 4–6 weeks, male and female)

were ordered from Charles River Laboratories International, Inc. All animal experiments were conducted in compliance with the guidelines for the care and use of research animals established by the University of Rhode Island Institutional Animal Care and Use Committee (IACUC).

Nanoparticle synthesis and formulation—HCuSNPs were synthesized according to previously reported method with minor modification.[33] Briefly, $CuCl_2$ solution (100 μL, 0.5 mol L^{-1}) was added to deionized water (25 mL) containing poly-(vinylpyrrolidone) (PVP-K40, 0.24 g) in a round flask under magnetic stirring at room temperature. Then, NaOH solution (25 mL, pH 9.0) was added, followed by addition of hydrazine anhydrous solution (6.4 μL) to form a suspension of Cu_2O spheres. After 5 min, Na_2S aqueous stock solution (200 μL, 320 mg/mL) was added to the suspension. The flask was heated for 2 h at 60°C. HCuSNPs were centrifuged at 11,000 rpm for 10 min at room temperature, and washed twice with distilled water.

HCuSNPs were resuspended in of solution containing Carbomer 940 (1 mL, 0.2%, Spectrum), and propylene glycol (10%) under magnetic stirring. The HCuSNP gel formed immediately after the addition of triethanolamine (2 μL). Blank gel was prepared without addition of HCuSNP.

In vivo laser activation—Nude mice were anesthetized and randomly divided into 3 groups (n=3 per group). The mice in Groups 1 and 2 received topical applications of HCuSNP gel (50 μL). The mice in Group 3 were applied with blank gel (50 μL). The mice are heated for 20 min using the light bulb in order that the water in gel can evaporate. Ten minutes after, a Q-switched Nd:YAG laser (LS-2137/2, LOTIS TII) in tandem with a tunable Ti:sapphire laser (LT-2211A, LOTIS TII) were employed to excite a zone of the gel-coated skin area for 5 s. The laser provided a pulse duration of less than 15 ns, a pulse repetition rate of 10 Hz, and a wavelength set at 900 nm. The spot size of the laser beam was adjusted to 6 mm in diameter. The laser power was calibrated using a Field Max II laser power/energy meter (Coherent). A laser power of 1.3 W/cm^2 was applied to the mice in Group 1, and 2.6 W/cm^2 to the mice in Groups 2 and 3. During laser irradiation, thermographs and temperature were recorded by an infrared camera (ICI7320, Infrared Camera Inc.). A circular region of interest (ROI) encompassing the irradiated tumor was drawn on thermographs and analyzed using IRFlash thermal imaging analysis software (Infrared Cameras Inc.).

Skin staining and histology—After laser activation, the gel on the skin was wiped with gauze. The mice were euthanized and the laser-activated skin was dissected for cryosectioning. The frozen slices (10 μm thickness) were stained with H&E and Nile red, respectively.[25] For Nile red staining, a stock solution containing Nile red in acetone (0.05%, w/v) was diluted with glycerol:water (75:25, v/v). A drop of the glycerol-dye solution (2.5 μg/mL) was applied to each tissue section and immediately covered with a coverslip. The slices were examined under an upright Zeiss Laser Scanning Confocal Microscope 510 (LSM510). Nile red was excited with the 488-nm argon laser line and visualized through a fluorescein filter set (450-to 490-nm excitation filter, 510-nm dichroic mirror, and 515-nm long pass emission filter).[25]

HCuSNP-mediated NIR laser-activated transdermal delivery of dextran-FITC and hGH—The anesthetized nude mice (n=3) were placed on the table with the abdomen facing up. The mice received topical applications of HCuSNP gel (50 μL) followed by NIR laser treatment for 5 s at 1.3 or 2.6 W/cm^2. The HCuSNPs were cleaned by gauze. Mouse skin pretreated with HCuSNP gel alone or blank gel plus laser was set as control groups.

Dextran-FITC (MW 20k) hydrogel (50 μL) containing dextran-FITC (50 μg/ml) and carboxymethylcellulose sodium (3%) was applied on the laser-activated area and covered with an adhesive covering to ensure skin contact throughout the study period. The gel was removed after 30 min and the applied skin area was washed under running water and blotted with lint-free tissue. The mice were then euthanized and the laser-activated skin was dissected for cryosectioning. The frozen slices (10 μm thickness) were examined directly under an upright fluorescence microscope (Nikon, Eclipse E600) with an FITC filter set.

In a parallel experiment, an hydrogel of hGH (0.2 mg/mL, 3H Biomedical) was prepared in phosphate buffer (50 mM, pH 7.5) containing sodium chloride (75 mM), and carboxymethylcellulose sodium (3%). The hGH gel (50 μL, 10 μg) was applied on the laser-activated area at time 0 and covered with an adhesive covering. The gel was removed after 3 h and the applied skin area was washed under running water and blotted with lint-free tissue. Animals were placed in a restrainer throughout the duration of the experiment. Blood samples were taken from the tail vein at 0, 0.5, 1, 2, 3, 4, and 6 h, respectively. Sera were separated using a centrifuge for 15 min at 3600 rpm and stored at −20°C until analysis. hGH concentrations were measured using an enzyme-linked immunosorbent assay (ELISA) commercial kit (Human Growth Hormone Diagnostic kit, BC2506, Immuno-Biological Laboratories, Inc.). Mice receiving s.c. injections of hGH aqueous solution (10 μg) was set as control. In group of transdermal delivery with chemical enhancer, mouse skin was directly applied with the above hGH gel containing Azone (5%) for 3 h. Areas under the concentration time curves from 0 to 6 h (AUC_{0-6h}) were calculated using a trapezoid method. Bioavailability of hGH through transdermal delivery relative to that via s.c. injection was calculated as follows:

$$\text{Bioavailability}\ (\%) = (AUC_{0-6h,\ t.d.}) / (AUC_{0-6h,\ s.c.}) \times 100 \quad (1)$$

where $AUC_{0-6h,\ t.d.}$ represents AUC of hGH from 0 to 6 h via transdermal delivery; $AUC_{0-6h,\ s.c.}$ represents AUC of hGH from 0 to 6 h via subcutaneous injection.

In vitro transdermal transport—The abdomen skin of nude mice was cut into small pieces with side length larger than 9 mm, which is the diameter of transport area of Franz diffusion cells (PermeGear Inc.). After the fat layer was carefully removed, the skin was divided into 6 groups (n=5). Skin in Groups 1 and 2 was applied with HCuSNP gel (50 μL) followed by NIR laser treatment with power intensity of 1.3 and 2.6 W/cm^2, respectively. In order to match the transport area of Franz diffusion cells, the laser light was expended through a concave lens (Thorlabs Inc.) to 9 mm in diameter. The laser power was calibrated by Field Max II laser power/energy meter. Skin in Groups 3 and 4 was pretreated with HCuSNP gel alone and NIR laser (2.6 W/cm^2) alone, respectively. The HCuSNPs were then removed by gauze. The pretreated skin in Groups 1–4 and the intact skin in Groups 5 and 6 was then mounted onto Franz diffusion cells with stratum corneum side facing upward. The receiver compartment contained 3 mL of PBS (pH 7.4) and was maintained at 37°C with a water circulator (Model 7306, PolyScience). The diffusion area of the skin was 0.64 cm^2. The donor compartment of Groups 1–5 was loaded with hGH in PBS (100 μg/mL, 250 μL, pH 7.4). The donor compartment of Group 6 was loaded with hGH in PBS (100 μg/mL, 250 μL, pH 7.4) containing Azone (5%). All donor compartments were covered with parafilm to prevent evaporation. At 0, 1, 2, 3, 4, 8, 12, and 24 h, samples (100 μL) were withdrawn from the receiver compartment and immediately replenished with fresh PBS. The drug concentration was measured by ELISA as described above. The following steady-state equation was used to calculate the permeability of the skin:

$$\text{Amount of drug permeated}\ (\mu g) = A \times C_0 \times K_p \times t \quad (2)$$

where, A is the diffusion area of the skin sample (0.64 cm^2), C_0 is the initial drug concentration in the donor chamber in μg/mL, K_p is the permeability to the drug in cm/h, and t is time in hours.

Skin irritation test—The mouse ear swelling test was used to evaluate the skin irritation of HCuSNPs according to the procedure described.[28] Briefly, BALB/c mice (n=5) were topically treated with either HCuSNP gel (20 mg/mL) or HCuSNPs in water (20 mg/mL) on the dorsal surface of each ear (50 μL per ear) once a day for three consecutive days. DNFB (0.3%) was used as positive control. Mouse ears without any treatment were used as negative control. The thickness of the right and left ear pinnae of each mouse was measured using a digital micrometer (Marathon Management) before the first application and 24 h following the final exposure. The mice were then euthanized and ears were dissected for frozen sectioning. Histological analysis was performed through H&E staining.

Acknowledgments

The authors acknowledge Dr. Robert Rodgers for editing the manuscript. This work was supported by grants from the National Center for Research Resources, the National Institutes of Health (RI-INBRE Award P20RR016457-10) and by the Rhode Island Foundation Medical Research Grant.

References

[1]. Prausnitz MR, Mitragotri S, Langer R. Nat. Rev. Drug Discov. 2004; 3:115–124. [PubMed: 15040576]

[2]. Prausnitz MR, Langer R. Nat. Biotechnol. 2008; 26:1261–1268. [PubMed: 18997767]

[3]. Elias PM, Choi EH. Exp. Dermatol. 2005; 14:719–726. [PubMed: 16176279]

[4]. Prausnitz MR. Adv. Drug Deliv. Rev. 2004; 56:581–587. [PubMed: 15019747]

[5]. a) Park JH, Lee JW, Kim YC, Prausnitz MR. Int. J. Pharm. 2008; 359:94–103. [PubMed: 18455889] b) Bramson J, Dayball K, Evelegh C, Wan YH, Page D, Smith A. Gene Ther. 2003; 10:251–260. [PubMed: 12571633] c) Birchall J, Coulman S, Anstey A, Gateley C, Sweetland H, Gershonowitz A, Neville L, Levin G. Int. J. Pharm. 2006; 312:15–23. [PubMed: 16469457] d) Levin G, Gershonowitz A, Sacks H, Stern M, Sherman A, Rudaev S, Zivin I, Phillip M. Pharm. Res. 2005; 22:550–555. [PubMed: 15846462] e) Fang JY, Lee WR, Shen SC, Wang HY, Fang CL, Hu CH. J. Control. Release. 2004; 100:75–85. [PubMed: 15491812] f) Bachhav YG, Summer S, Heinrich A, Bragagna T, Bohler C, Kalia YN. J. Control. Release. 2010; 146:31–36. [PubMed: 20678988]

[6]. Glenn GM, Flyer DC, Ellingsworth LR, Frech SA, Frerichs DM, Seid RC, Yu J. Expert Rev. Vaccines. 2007; 6:809–819. [PubMed: 17931160]

[7]. Zhao YL, Murthy SN, Manjili MH, Guan LJ, Sen A, Hui SW. Vaccine. 2006; 24:1282–1290. [PubMed: 16225969]

[8]. Ogura M, Paliwal S, Mitragotri S. Adv. Drug Deliv. Rev. 2008; 60:1218–1223. [PubMed: 18450318]

[9]. Hirsch LR, Stafford RJ, Bankson JA, Sershen SR, Rivera B, Price RE, Hazle JD, Halas NJ, West JL. Proc. Natl. Acad. Sci. U S A. 2003; 100:13549–13554. [PubMed: 14597719]

[10]. Dickerson EB, Dreaden EC, Huang X, El-Sayed IH, Chu H, Pushpanketh S, McDonald JF, El-Sayed MA. Cancer Lett. 2008; 269:57–66. [PubMed: 18541363]

[11]. Skrabalak SE, Chen J, Au L, Lu X, Li X, Xia Y. Adv. Mater. 2007; 19:3177–3184. [PubMed: 18648528]

[12]. Lu W, Xiong C, Zhang G, Huang Q, Zhang R, Zhang JZ, Li C. Clin. Cancer Res. 2009; 15:876–886. [PubMed: 19188158]

[13]. O'Neal DP, Hirsch LR, Halas NJ, Payne JD, West JL. Cancer Lett. 2004; 209:171–176. [PubMed: 15159019]

[14]. Weissleder R. Nat. Biotechnol. 2001; 19:316–317. [PubMed: 11283581]

[15]. a) Lal S, Clare SE, Halas NJ. Acc. Chem. Res. 2008; 41:1842–1851. [PubMed: 19053240] b) Huang X, El-Sayed IH, El-Sayed MA. Methods Mol. Biol. 2010; 624:343–357. [PubMed: 20217607] c) Hu M, Chen JY, Li ZY, Au L, Hartland GV, Li XD, Marquez M, Xia YN. Chem. Soc. Rev. 2006; 35:1084–1094. [PubMed: 17057837] d) Melancon MP, Zhou M, Li C. Acc. Chem. Res. 2011; 44:947–956. [PubMed: 21848277]

[16]. a) You J, Zhang G, Li C. ACS Nano. 2010; 4:1033–1041. [PubMed: 20121065] b) Kuo TR, Hovhannisyan VA, Chao YC, Chao SL, Chiang SJ, Lin SJ, Dong CY, Chen CC. J. Am. Chem. Soc. 132:14163–14171. [PubMed: 20857981] c) Wu G, Mikhailovsky A, Khant HA, Fu C, Chiu W, Zasadzinski JA. J. Am. Chem. Soc. 2008; 130:8175–8177. [PubMed: 18543914]

[17]. a) Wijaya A, Schaffer SB, Pallares IG, Hamad-Schifferli K. ACS Nano. 2009; 3:80–86. [PubMed: 19206252] b) Chen CC, Lin YP, Wang CW, Tzeng HC, Wu CH, Chen YC, Chen CP, Chen LC, Wu YC. J. Am. Chem. Soc. 2006; 128:3709–3715. [PubMed: 16536544]

[18]. a) Braun GB, Pallaoro A, Wu G, Missirlis D, Zasadzinski JA, Tirrell M, Reich NO. ACS Nano. 2009; 3:2007–2015. [PubMed: 19527019] b) Lu W, Zhang G, Zhang R, Flores LG 2nd, Huang Q, Gelovani JG, Li C. Cancer Res. 2010; 70:3177–3188. [PubMed: 20388791]

[19]. Pissuwan D, Nose K, Kurihara R, Kaneko K, Tahara Y, Kamiya N, Goto M, Katayama Y, Niidome T. Small. 2011; 7:215–220. [PubMed: 21213384]

[20]. a) Liz-Marzan LM. Langmuir. 2006; 22:32–41. [PubMed: 16378396] b) Zhang JZ, Noguez C. Plasmonics. 2008; 3:127–150.

[21]. Li Y, Lu W, Huang Q, Huang M, Li C, Chen W. Nanomedicine (Lond). 2010; 5:1161–1171. [PubMed: 21039194]

[22]. Jain PK, Lee KS, El-Sayed IH, El-Sayed MA. J. Phys. Chem. B. 2006; 110:7238–7248. [PubMed: 16599493]

[23]. a) Tian Q, Tang M, Sun Y, Zou R, Chen Z, Zhu M, Yang S, Wang J, Hu J. Adv. Mater. 2011; 23:3542–3547. [PubMed: 21735487] b) Song S, Xiong C, Zhou M, Lu W, Huang Q, Ku G, Zhao J, Flores LG Jr. Ni Y, Li C. J. Nucl. Med. 2011; 52:792–799. [PubMed: 21498539]

[24]. Zhou M, Zhang R, Huang M, Lu W, Song S, Melancon MP, Tian M, Liang D, Li C. J. Am. Chem. Soc. 2010; 132:15351–15358. [PubMed: 20942456]

[25]. Talreja P, Kleene NK, Pickens WL, Wang TF, Kasting GB. AAPS PharmSci. 2001; 3:E13. [PubMed: 11741264]

[26]. Kim J, Park S, Lee JE, Jin SM, Lee JH, Lee IS, Yang I, Kim JS, Kim SK, Cho MH, Hyeon T. Angew. Chem. 2006; 118:7918–7922. *Angew. Chem. Int. Ed. Engl.* 2006, 45, 7754-7758.

[27]. a) Lee JW, Gadiraju P, Park JH, Allen MG, Prausnitz MR. J. Control. Release. 2011; 154:58–68. [PubMed: 21596072] b) Yu J, Kalaria DR, Kalia YN. J. Control. Release. 2011; 156:53–59. [PubMed: 21803083]

[28]. Anderson SE, Umbright C, Sellamuthu R, Fluharty K, Kashon M, Franko J, Jackson LG, Johnson VJ, Joseph P. Toxicol. Sci. 2010; 115:435–443. [PubMed: 20176622]

[29]. a) Pitsillides CM, Joe EK, Wei X, Anderson RR, Lin CP. Biophys. J. 2003; 84:4023–4032. [PubMed: 12770906] b) Hu M, Hartland GV. J. Phys. Chem. B. 2002; 106:7029–7033.

[30]. Link S, Hathcock DJ, Nikoobakht B, El-Sayed MA. Adv. Mater. 2003; 15:393–396.

[31]. Hoogstraate AJ, Verhoef J, Brussee J, Ijzerman AP, Spies F, Bodde HE. Int. J. Pharm. 1991; 76:37–47.

[32]. Glenn GM, Kenney RT. Curr. Top. Microbiol. Immunol. 2006; 304:247–268. [PubMed: 16989274]

[33]. Zhu H, Wang J, Wu D. Inorg. Chem. 2009; 48:7099–7104. [PubMed: 19585979]

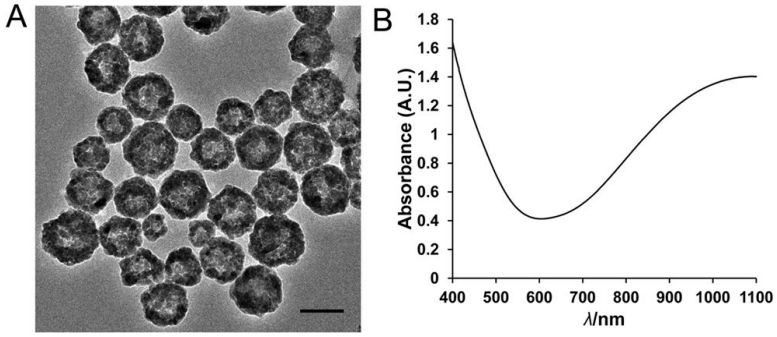

Figure 1.

A) Transmission electron micrograph of HCuSNPs. B) Experimental absorbance spectrum of HCuSNPs in water. Bar, 50 nm.

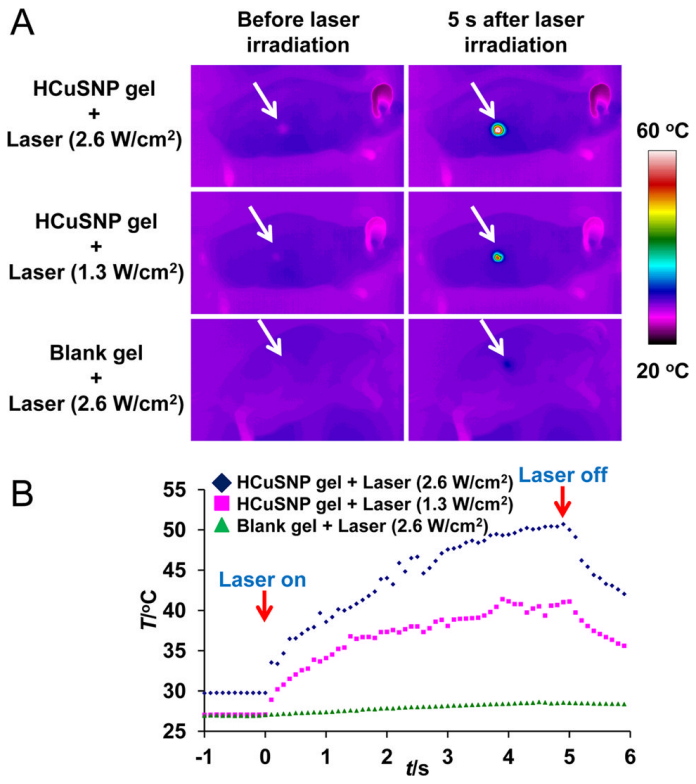

Figure 2.

A) Thermographic images of nude mice under the NIR laser treatment. Nude mice received 50 μL of gel with or without HCuSNPs followed by NIR laser irradiation. Arrows, skin area treated with gel and laser. B) Plots of average temperature in the laser-shining area as a function of irradiation time.

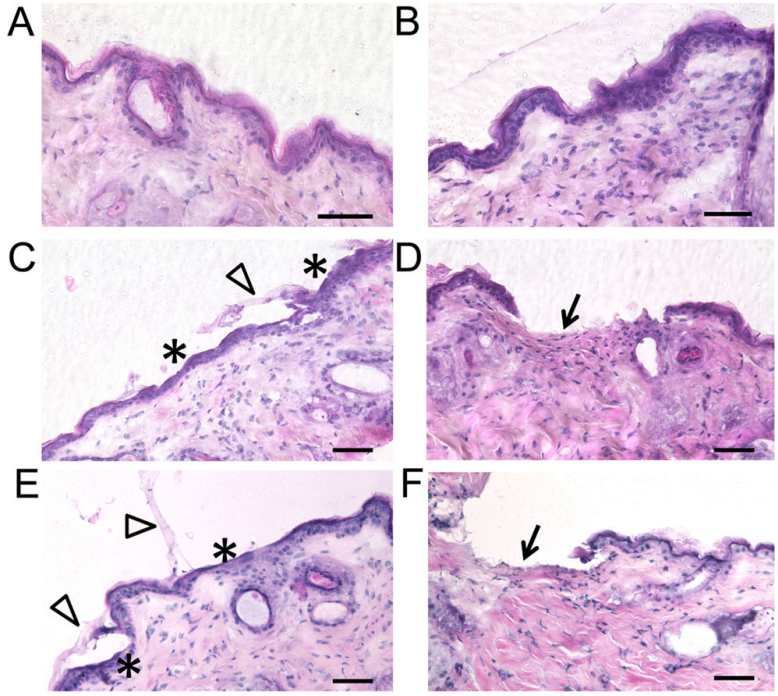

Figure 3.

H&E staining of the skin sections from the anesthetic nude mice pretreated with A) HCuSNP gel, B) blank gel plus laser (2.6 W/cm^2), C) HCuSNP gel plus laser (1.3 W/cm^2), D) HCuSNP gel plus laser (2.6 W/cm^2), E) HCuSNP solution plus laser (1.3 W/cm^2), or F) HCuSNP solution plus laser (2.6 W/cm^2). Asterisks, epidermis without stratum corneum; Arrowheads, stratum corneum layers stripped from epidermis; Arrows, dermis with removal of both stratum corneum and viable epidermis. Bars, 50 μm.

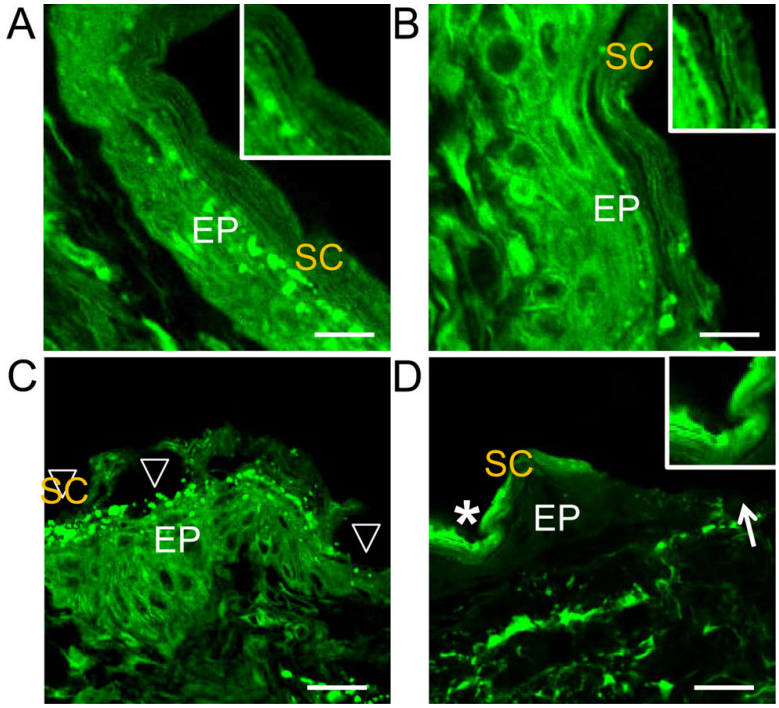

Figure 4.

Representative Nile red staining of the skin sections from the anesthetic nude mice pretreated with A) HCuSNP gel, B) blank gel plus laser (2.6 W/cm^2), C) HCuSNP gel plus laser (1.3 W/cm^2), or D) HCuSNP gel plus laser (2.6 W/cm^2). EP, epidermis; SC, stratum corneum; Arrowheads, epidermis without stratum corneum; Asterisk, densely packed stratum corneum; Arrow, loss of epidermis. Inner graphs are the enlargement of the stratum corneum area. Bars, A) and B) 10 μm; C) and D) 20 μm.

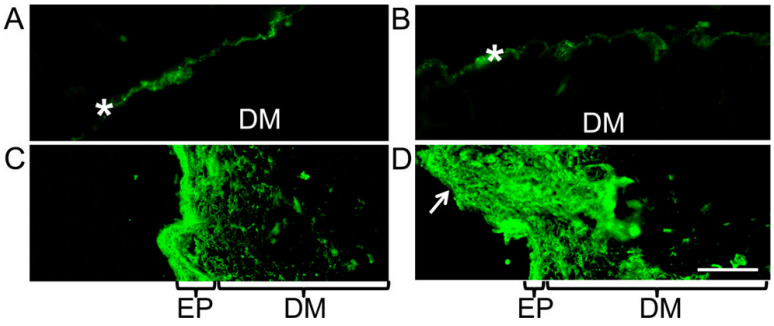

Figure 5.

Fluorescence micrographs of the dextran-FITC (MW 20 k)-applied skin sections from the anesthetic nude mice pretreated with A) HCuSNP gel, B) blank gel plus laser (2.6 W/cm^2), C) HCuSNP gel plus laser (1.3 W/cm^2), or D) HCuSNP gel plus laser (2.6 W/cm^2). EP, epidermis; DM, dermis; Asterisks, stratum corneum; Arrow, loss of epidermis. Bar, 100 μm.

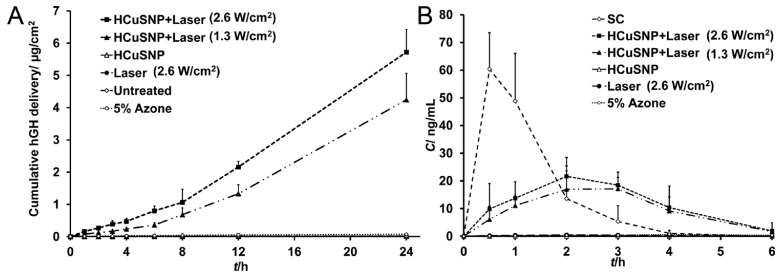

Figure 6.

A) Cumulative delivery of hGH solution across nude mouse skin pretreated with HCuSNP gel alone, laser alone, or HCuSNP gel with laser. “Untreated” group, the intact skin without pretreatment. “5% Azone” group, hGH solution containing 5% Azone was applied to the intact skin without pretreatment. Each value represents Mean ± S.D. (n=5). B) hGH levels in serum after s.c. injection or transdermal delivery with different pretreatment, at a dose of 10 μg hGH. For transdermal delivery, hGH gel was applied to the skin for 3 h starting at time 0. In “5% Azone” group, hGH gel containing 5% Azone was directly applied to the intact mice skin without pretreatment. Each data point represents the mean ± SD of 3 nude mice.

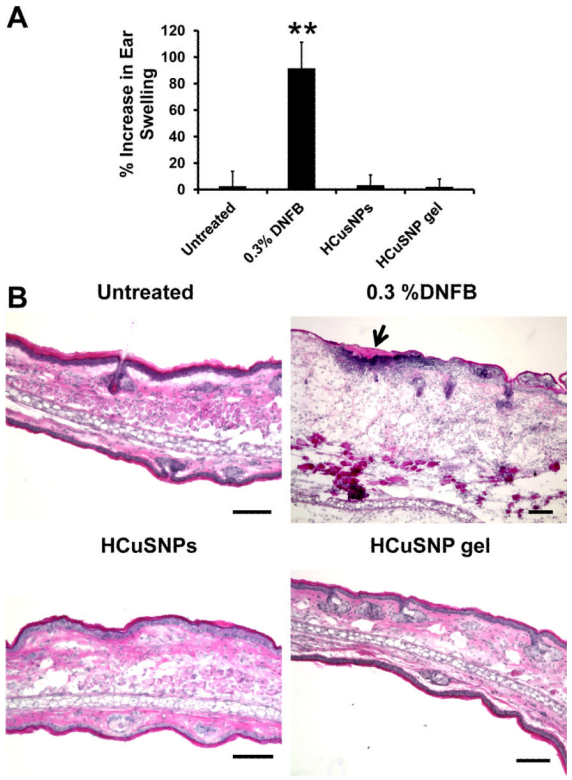

Figure 7.

A) Ear swelling as a result of topical application of different agents through measurement of the increase of thickness of ear pinnae before and after treatment. Bars represent Mean ± SD of five mice (10 ears) per group. **, $p < 0.01$ as compared to other groups. B) Representative histology of ear skin following different treatment by H&E staining. Top side was the application site. Arrow represents area of dermatitis, i.e. squamous cell hyperplasia and polymorphonuclear cell infiltration at the application site. Bar, 100 μm.

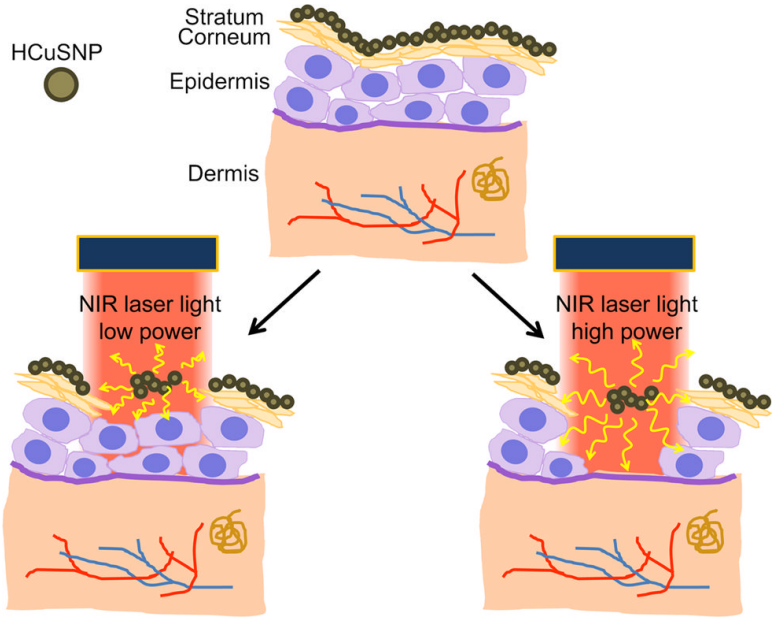

Scheme 1.
Illustration of NIR laser-triggered photothermal ablation of skin mediated by HCuSNPs.